Magnesium Technology 2011
Edited by: Wim H. Sillekens, Sean R. Agnew, Neale R. Neelameggham, and Suveen N. Mathaudhu
TMS (The Minerals, Metals & Materials Society), 2011

EFFECT OF HEAT INDEX ON MICROSTRUCTURE AND MECHANICAL BEHAVIOR OF FRICTION STIR PROCESSED AZ31

Wei Yuan, Rajiv S. Mishra
Center for Friction Stir Processing, Department of Materials Science and Engineering
Missouri University of Science and Technology, Rolla, MO 65409, USA

Keywords: friction stir processing, heat index, tensile behavior, anisotropy, work hardening

Abstract

Friction stir processing modifies the microstructure and properties of metals through intense plastic deformation. The frictional heat input affects the microstructure evolution and resulting mechanical properties. 2 mm thick commercial AZ31B-H24 Mg alloy was friction stir processed under various process parameter combinations to investigate the effect of heat index on microstructure and properties. Recrystallized grain structure in the nugget region was observed for all processing conditions with decrease in hardness. Results indicate a reduced tensile yield strength and ultimate tensile strength compared to the as-received material in H-temper, but with an improved hardening capacity. The strain hardening behavior of friction stir processed material is discussed.

Introduction

Friction stir processing (FSP), a derivate from friction stir welding [1], has emerged as an effective tool for microstructural modification. During FSP, a non-consumable rotating tool plunges into the workpiece and traverses along a pre-determined direction. FSP locally modifies the microstructure by refining the grain structure and homogenizing any precipitate particles as a result of severe plastic deformation and dynamic recrystallization [2-3]. The tool rotation rate (ω) and traverse speed (υ) play a key role in frictional heat generation and afterward heat dissipation, which dominate the microstructure evolution. It is generally accepted that higher tool rotation rate or a lower tool traverse speed produces more frictional heat. A higher tool traverse speed is beneficial for achieving higher heat dissipation, i.e., higher cooling rate [4].

It has been shown that reducing the frictional heat and increasing the heat dissipation rate are beneficial for grain refinement during FSP of magnesium alloys [5-8]. However, it is difficult to quantify the heat input during FSP due to the parameter variables and materials to be processed. Arbegast and Hartley [9] established an empirical relationship for aluminum alloys between the nugget temperature and the processing parameters based on experimental observations, the pseudo heat index (HI) $\omega^2/\upsilon*10^{-4}$, expressed by $T/T_m=K(\omega^2/\upsilon*10^{-4})^{\alpha}$, where T_m is melting point, K is a constant between 0.65 and 0.75, and α varies from 0.04 to 0.06.

The present work seeks to investigate the effect of heat index on microstructure evolution and mechanical properties of FSPed magnesium alloy AZ31. Tensile testing was performed to characterize the anisotropy and work hardening behavior of FSPed AZ31 in nugget region.

Experimental Procedure

A commercial grade AZ31-H24 magnesium alloy having a thickness of 2.0 mm was used. To make friction stir passes, a tool with 12 mm diameter concave shoulder and 1.5 mm conical pin was employed. FSP of AZ31 was carried out at various process parameters as shown in Table 1. Tensile properties were characterized by using mini-tensile specimens having a gage length of 1.3 mm, a width of 1.0 mm, and a thickness of 0.6 mm. Samples were machined along the processing direction (PD) and transverse direction (TD) from the center of the nugget as shown in Figure 1, and were polished with 1 μm finish and tested at room temperature at a strain rate of 1×10^{-3} s^{-1}. Microhardness measurements were performed at the middle of the nugget center line with a 0.5 kgf load and 10 s dwell time. Five hardness values were obtained for each heat index condition. Microstructure of FSP samples, cross-section perpendicular to the PD, was examined using optical microscopy. Samples were mechanically polished to 1μm and etched using an acetic picral solution (4.2 g picric acid, 10 ml acetic acid, 10 ml water, and 70 ml ethanol). The linear intercept method was used to obtain an average grain size.

Table I. A summary of process parameters were used in this study.

ω (rpm*100)	5	6	6	6	6	6	6	7	8	9
υ (ipm)	2	2	4	6	8	10	12	2	2	2

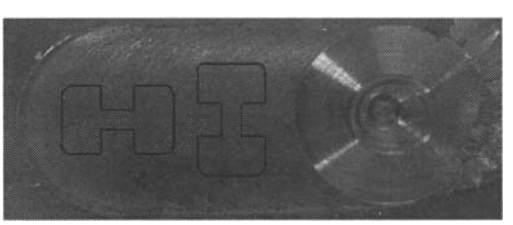

Figure 1. Friction stir processed AZ31 with mini-tensile specimen arrangement.

Results and Discussion

Microstructure Evolution

Figure 2(a) presents the microstructure of as-received AZ31 alloy. The most dominant feature of this microstructure is heavily twinned grains which is consistent with the H temper of as-received material. Figures 2(b) to 2(d) show the nugget microstructures of FSPed AZ31 at various processing conditions. Compared with the as-received material, more uniform grain structures were achieved because of dynamic recrystallization and grain growth. The variation in grain size among the three processing conditions is obvious. A fine grain structure with an average grain size of 3.8±0.6 μm was achieved at a tool rotation rate of 600 revolutions per minute (rpm) and a tool traverse speed

of 8 inches per minute (ipm). However, a relatively coarse grain structure was produced at 900 rpm and 2 ipm with an average grain size of 10.2±2.2 μm. The grain size of the nugget at 600 rpm and 2 ipm was 6.0±1.5 μm.

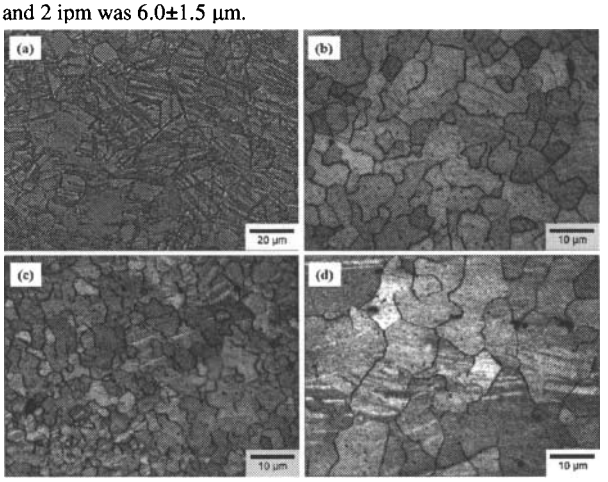

Figure 2. Microstructure of AZ31 alloy in (a) as-received condition, (b) FSPed at 600 rpm and 2 ipm, (c) FSPed at 600 rpm and 8 ipm, and (d) FSPed at 900 rpm and 2 ipm.

The grain size of nugget varied with processing condition or the heat index. The grain structure evolution of magnesium alloys during FSP is complex and generally accepted as a result of dynamic recrystallization [10-12]. The average grain size in the nugget is plotted against heat index in Figure 3. For this particular alloy and tool used, the grain size appears to vary linearly with the heat index; grain size increases with the heat index. A finest grain structure with an average grain size of 3.1 μm was achieved at a heat index of 3.6. On the other hand, a coarsest grain structure with an average grain size of 10.2 μm was achieved at a heat index of 40.5. It has been reported that an increase in tool rotation rate or a decrease in tool traverse speed leads to an increase in grain size [13].

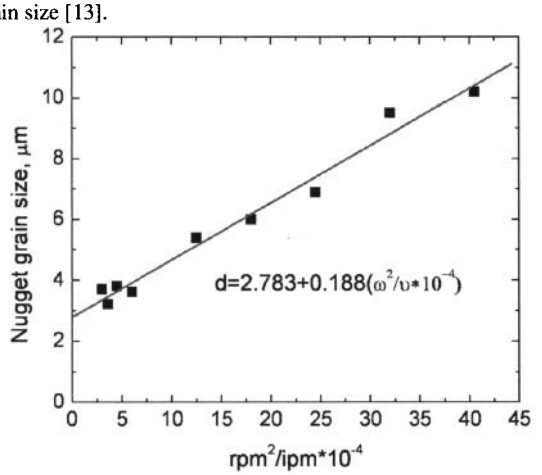

Figure 3. Variation of average nugget grain size with heat index.

Mechanical Behavior

Figure 4(a) shows the plot of microhardness at middle region of the nugget. The hardness of nugget decreases after FSP as compared to the as-received material, which is ~70 HV. Within the heat indices used, the hardness first decreases from about 62 HV to 53 HV as the heat index increases from 4.5 to 12.5, and then stays almost constant. The hardness of the nugget is dominated by grain size and dislocation density, since AZ31 magnesium alloy does not have significant level of precipitates for strengthening. The as-received AZ31 was in work-hardened condition. The stored dislocations and twins contribute to the relatively higher hardness value. On the other hand, the FSPed AZ31 exhibits a fully recrystallized microstructure. The hardness variation indicates that the grain size plays an important role when the average size is below 5 μm. Yang et al. [14] reported that the hardness values of friction stir welded AZ31 did not change much when the grain size was larger than 10 μm. Figure 4(b) presents the relationship between microhardness and average grain size in the nugget region. The Hall-Petch relationship between the hardness and the nugget grain size is observed when the nugget grain size is larger than 5 μm, however, data points with grain sizes less than 4 μm deviate from this expression. Combined with the previous results of FSPed fine grain structure with grain size in the range of 1 to 3 μm, the highest hardness values for the present work fit the Hall-Petch equation reported as $HV=33.3+58.6d^{-1/2}$ [7]. Though Chang et al. [15] reported a single slope for Hall-Petch relationship for FSPed AZ31 with a wide grain size range (3 to 100 μm), the current results indicate an inconsistency when the grain size is between 3 and 5 μm.

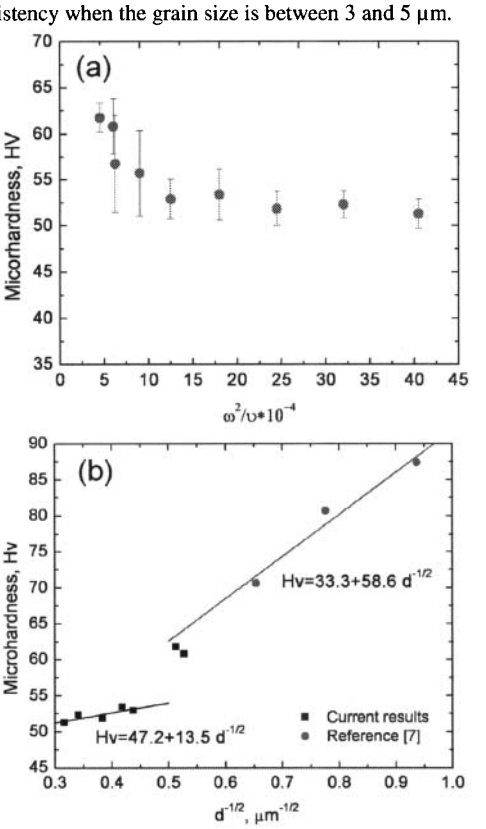

Figure 4. Microhardness variation as a function of (a) heat index, and (b) nugget grain size.

Figure 5 presents room temperature tensile stress-strain curves at a strain rate of $1x10^{-3}$ s^{-1} for the as-received and FSPed AZ31 alloy at four different heat indices 4.5, 18 and 40.5, along two

orthogonal directions; the RD for as-received AZ31alloy or the PD for FSPed AZ31 alloy, and the TD for all. Mini-tensile results of the as-received AZ31 alloy exhibited minor anisotropic behavior evidenced by slightly higher strength in the TD. The FSPed AZ31 alloy exhibited significant anisotropic behavior with higher strength but lower ductility in the TD as compared to the PD. The yield strength of the sample tested in the PD decreased from 243 MPa to about 110 MPa, 74 MPa and 50 MPa for heat index at 4.5, 18 and 40.5, respectively. For samples tested in the TD, the yield strength decreased from 274 MPa to about 233 MPa, 213 MPa and 170 MPa, respectively. The specimens tested in PD showed higher ductility and uniform elongation than those of TD. These results are different from the previous results for FSPed ultra-fine grained AZ31, which showed both higher strength and ductility in TD than PD [8].

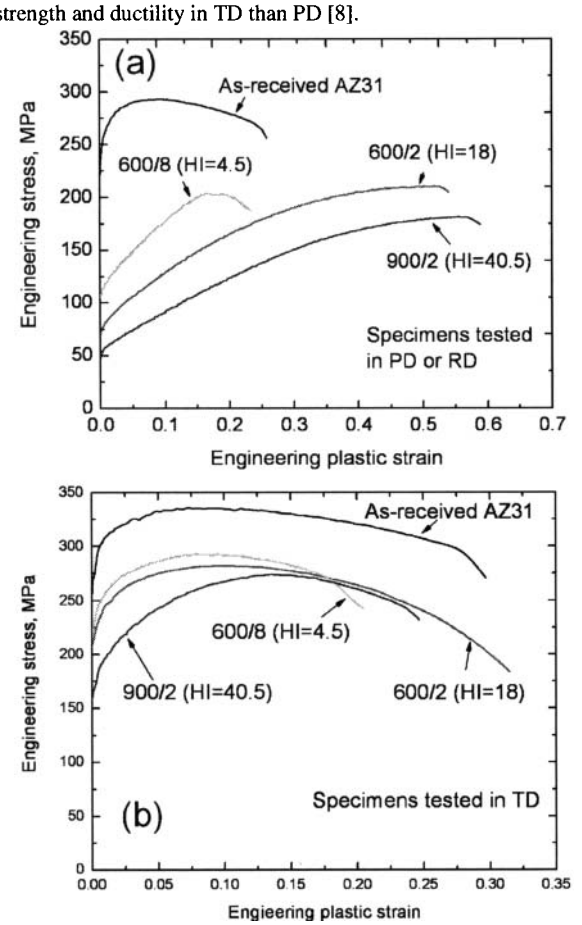

Figure 5. Stress - plastic strain curves for AZ31 alloy tested in (a) processing or rolling direction and (b) transverse direction.

The significant anisotropy in tensile behavior was related to the unique fiber texture generation in the nugget during FSP, where the tilt of basal poles was depth dependent. The tilt of basal poles in the center line of the nugget increased as the depth increased. At a location of 75% of the nugget depth, the basal poles were roughly parallel to the PD [8]. For the current results, the basal poles are expected to have a similar character, which favors the basal plane slip during tensile test when the loading axis is along the PD, indicated by much lower tensile yield strength in Figure 5(a). The difference in the yield strength among various heat indices is related to the variation in the grain size. As the heat index decreases, the average grain size becomes lower, so a higher stress is required for plastic deformation to occur for a similar texture. The yield strength shows similar trend when specimens were tested along TD, it increases as the indices decreases. The stress-strain curves also indicate that the uniform elongation increases as the grain size increases from 3.8 μm to 10.2 μm, which could be related to the twinning effect [16].

Figure 6 shows the degree of anisotropy in yield strength between TD and PD or (RD for as-received AZ31 alloy). The as-received AZ31 alloy exhibited low anisotropy with a difference of about 32 MPa in the yield strength. However, the degree of anisotropy for FSPed AZ31 alloy was significant and a difference of about 120 MPa in yield strength was noted. A ratio of difference in yield strength to the maximum tensile yield strength was also plotted. The ratio decreases as the heat index decreases, i.e., the ratio decreases with the grain size. As the grain size decreases to a critical scale, non-basal slip systems can be activated even at room temperature [17,18], which should reduce the anisotropy.

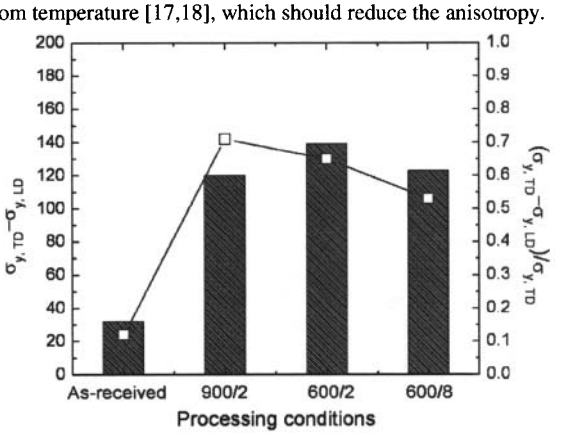

Figure 6. Degree of anisotropy at various processing conditions.

The hardening capacity, H_c, defined as a ratio of the ultimate tensile strength to the yield strength, signifies the capacity to which the material can be strain-hardened [19]. H_c is plotted for AZ31 alloy for various heat indices and compared to the as-received condition in Figure 7. A significant increase in hardening capacity can be observed for the specimens tested in PD. Similar results were reported by Afrin et al. [20] and Chowdhury et al. [21]. On the other hand the increase in hardening capacity is not obvious for TD. As defined, the hardening capacity of a material is directly related to its yield strength and the following strain hardening contributed by dislocation-dislocation interaction and interaction of dislocation with other microstructural features, such as twin boundaries. The as-received AZ31 alloy was in cold-worked and partially annealed condition. With the pre-existence dislocations and twinning, the yield strength was high and the hardening capacity low. However, FSPed AZ31 shows a dynamic recrystallized grain structure with a relatively lower dislocation density [14]. An increase in heat index or grain size decreases the tensile yield strength, but increases the ability of dislocation storage in a grain [19]. This explains the relatively higher hardening capacity at a higher HI. Texture also plays a role in hardening capacity; the higher hardening capacity is also related to the activation of easier basal slip system. Compared with the as-received AZ31, which has a harder texture (low Schmid factor) for basal slip for in-plane tensile tests, the specimens tested in PD

for FSPed AZ31 have a softer texture (high Schmid factor) for basal slip. The texture effect on hardening capacity can be seen from the different behaviors between TD and PD. A much reduced hardening capacity is observed for TD due to the harder texture for basal slip, which requires higher stress to activate the non-basal slip systems or twinning.

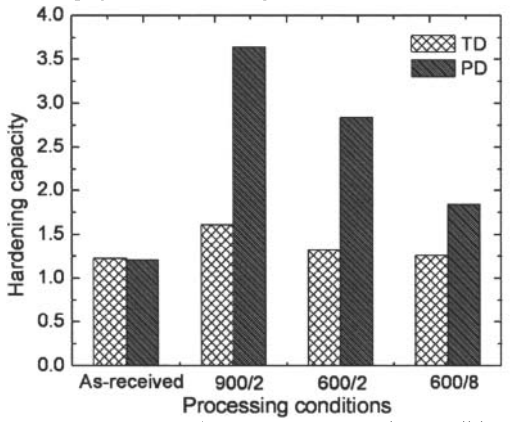

Figure 7. Hardening capacity at various processing conditions.

Figure 8 plots the work hardening rate derived from true stress vs. true strain as a function of net flow stress for various heat indices for both PD and TD. For the specimens tested in PD or RD (Figure 8(a)), the work hardening rate decreases steadily with the increase of flow stress during the initial stage due to the balance between storage and annihilation of dislocations, which is the stage III hardening range [22]. The as-received AZ31 alloy shows a higher work hardening rate than FSPed AZ31 during the initial period and extend of work hardening period is short. The initial drop in work hardening rate for FSPed AZ31 is followed by an increase when the net flow stress exceeds 30 MPa and subsequent decrease again. Similar work hardening phenomenon has been reported by Lee et al. [23]. They suggested that in addition to the texture effect, the increased work hardening rate should be correlated with the deformation-twin induced grain refinement and intense stress concentration as a result of interaction between dislocation and twin. The current results also indicate that the grain size influences the work hardening rate. At same net flow stress, the work hardening rate decreases as the heat index or grain size increases. The increase in work hardening rate after stage III is more prominent for larger grain size material, which may due to easier twinning in larger grains [16]. Figure 8(b) exhibits the work hardening rate for specimens tested in TD. A much higher initial work hardening rate is observed for TD compared to PD for FSPed AZ31 alloy. The difference in hardening behavior could be related to different deformation mechanisms introduced by texture. A key difference is that the intermediate stage of increase in work hardening rate is not observed in TD specimens. The FSPed finer grain AZ31 shows higher work hardening rate at initial hardening stage, but lower work hardening rate at higher net flow stress region. Sinclair et al. [24] and Kovacs et al. [25] reported that grain size strongly influenced strain hardening at lower strains, and the influence diminishes at higher strains due to dislocation screening and dynamic recovery effects at grain boundaries. Recently, de Valle et al. [26] reported that decreasing the grain size resulted in a decrease in work hardening rate in rolled and annealed AZ31 (grain size range of 2 to 55 μm). However, current results indicate that grain size influences work hardening differently when texture effect is superimposed.

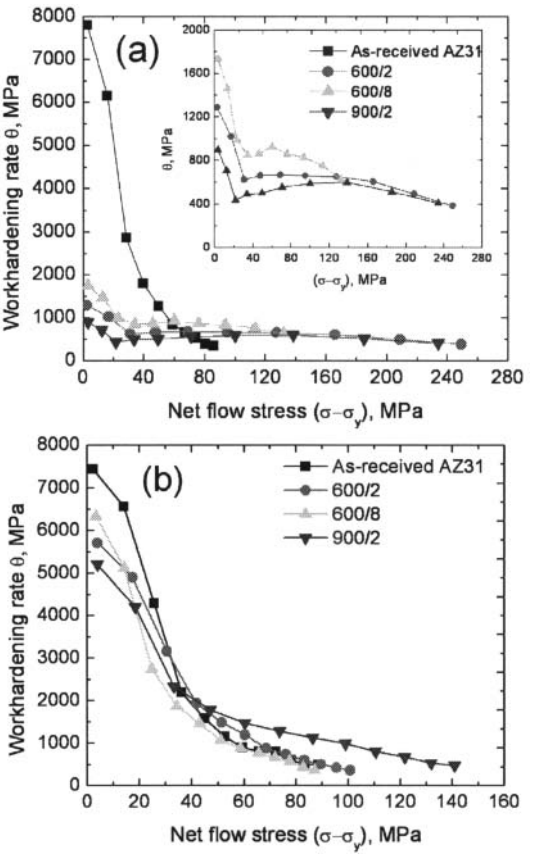

Figure 8. Work hardening rate derived from true stress vs. true strain (considering only uniform elongation), for various processing conditions, tested in (a) PD and (b) TD.

Conclusions

Friction stir processing modifies the microstructure and properties of metals through intense plastic deformation. The frictional heat index exhibits a great effect on the dynamically recrystallized grain structure in the nugget and resulting mechanical properties. Results indicate that nugget grain size increases linearly with the heat index, which in turn reduces the nugget hardness, tensile yield strength, but improves the work hardening capacity. The anisotropy in tensile behavior in transverse direction and processing direction is related to the unique fiber texture generated in the nugget. Both the texture and grain size have a great effect on work hardening behavior. For specimens tested in PD, the finer the grain size, the higher the work hardening rate; however, for specimens tested in TD, the finer grain size exhibits higher work hardening rate only at lower net flow stress stage, but lower work hardening rate at higher net flow stress region.

Acknowledgements

The authors gratefully acknowledge the support of the National Science Foundation through grant NSF-EEC-0531019.

References

[1] W.M. Thomas, E.D. Nicholas, J.C. Needham, M.G. Murch, P. Templesmith, C. J. Dawes, G.B. Patent 9125978.8 (1991).
[2] R.S. Mishra, M.W. Mahoney, S.X. McFadden, N.A. Mara, A.K. Mukherjee, *Scr. Mater.*, 42 (1999) 163-168.
[3] R.S. Mishra and Z.Y. Ma, "Friction stir welding and processing," *Mater. Sci. Eng. R: Reports*, 50 (2005) 1-78.
[4] L. Cui et al., "Friction stir welding of a high carbon steel," *Scr. Mater.*, 56 (2007), 637-640.
[5] C.I. Chang, X.H. Du, J.C. Huang, "Achieving ultrafine grain size in Mg-Al-Zn alloy by friction stir processing," *Scr. Mater.*, 57 (2007) 209-212.
[6] C.I. Chang et al., "Producing nanograined microstructure in Mg–Al–Zn alloy by two-step friction stir processing," *Scr. Mater.*, 59 (2008), 356-359.
[7] G. Bhargava et al., "Influence of texture on mechanical behavior of friction-stir-processed magnesium alloy," *Metall. Mater. Trans.*, 41 (2010) 13-17.
[8] W. Yuan et al., "Effect of texture on the mechanical behavior of ultra-fine grained magnesium Alloy," to be submitted to Scr. Mater..
[9] W.J. Arbegast, P.J. Hartley, in: Proceedings of the Fifth International Conference of Trends in Welding Research, Pine Mountain, GA, June 1–5, 1998, p. 541.
[10] J.A. Esparza et al.," Friction-stir welding of magnesium alloy AZ31B," *J. Mater. Sci. Lett.*, 21 (2002) 917-920.
[11] S.H.C. Park, Y.S. Sato, H. Kokawa, "Microstructural evolution and its effect on Hall-Petch relationship in friction stir welding of thixomolded Mg alloy AZ91D," J. *Mater. Sci.*, 38 (2003) 4379-4383.
[12] W.B. Lee, Y.M. Yeon, S.B. Jung, "Joint properties of friction stir welded AZ31B - H24 magnesium alloy," Mater. Sci. Technol., 19 (2003) 785-790.
[13] L. Commin et al., "Friction stir welding of AZ31 magnesium alloy rolled sheets: Influence of processing parameters," *Acta Mater.*, 57 (2009) 326-334.
[14] J. Yang et al., "Effects of heat input on tensile properties and fracture behavior of friction stir welded Mg-3Al-1Zn alloy," *Mater. Sci. Eng. A*, 527 (2010) 708-714.
[15] C.I. Chang et al., "Relationship between grain size and Zener–Holloman parameter during friction stir processing in AZ31 Mg alloys," *Scr. Mater.*, 51 (2004), 509-514.
[16] M.R. Barnett et al., "Influence of grain size on the compressive deformation of wrought Mg-3Al-1Zn," *Acta Mater.*, 52 (2004) 5093-5103.
[17] J. Koike et al., "The activity of non-basal slip systems and dynamic recovery at room temperature in fine-grained AZ31B magnesium alloys," *Acta Mater.*, 51 (2003) 2055-2065.
[18] S.R. Agnew and O. Duygulu, "Plastic anisotropy and the role of non-basal slip in magnesium alloy AZ31B," *Int. J. Plast.*, 21 (2005) 1161-1193.
[19] J. Luo et al., "Diminishing of work hardening in electroformed polycrystalline copper with nano-sized and uf-sized twins," *Mater. Sci. Eng. A*, 441 (2006) 282-290.
[20] N. Afrin et al., "Strain hardening behavior of a friction stir welded magnesium alloy," *Scr. Mater.*, 57 (2007) 1004-1007.
[21] S.M. Chowdhury et al., "Tensile properties and strain-hardening behavior of double-sided arc welded and friction stir welded AZ31B magnesium alloy," *Mater. Sci. Eng. A*, 527 (2010) 2951-2961.
[22] U.F. Kocks and H. Mecking, "Physics and phenomenology of strain hardening: the FCC case," *Prog. Mater. Sci.*, 48 (2003) 171-273.
[23] H.-W. Lee et al., "Studies on the improvement of tensile ductility of hot-extrusion AZ31 alloy by subsequent friction stir process," *J. Alloys Compd.*, 475 (2009) 139-144.
[24] C.W. Sinclair et al., "A model for the grain size dependent work hardening of copper," *Scr. Mater.*, 55 (2006), 739-742.
[25] I. Kovacs et al., "Grain size dependence of the work hardening process in Al99.99," Phys. Status Solidi A 194 (2002) 3-18.
[26] J.A. del Valle et al., "Influence of texture and grain size on work hardening and ductility in magnesium-based alloys processed by ECAP and rolling," *Acta Mater.*, 54 (2006) 4247-4295.